The Influence of Annealing Treatment on the Molecular Structure and the Mechanical Properties of Isotactic Polypropylene Fibers

Ismail Karacan,[1] Hüseyin Benli[2]

[1]*Department of Textile Engineering, Erciyes University, Kayseri, Turkey*
[2]*Mustafa Çıkrıkçıoğlu Vocational School, Erciyes University, Kayseri, Turkey*

Received 11 January 2011; accepted 21 February 2011
DOI 10.1002/app.34440
Published online 12 July 2011 in Wiley Online Library (wileyonlinelibrary.com).

ABSTRACT: An investigation was carried out on the effects of annealing treatment on the molecular structure and the mechanical properties of isotactic polypropylene fibers annealed in an air heated environment at temperatures ranging from 60 to 140°C. Analysis of the equatorial X-ray diffraction traces showed the presence of a three phase system of amorphous-smectic-monoclinic forms and revealed the transformation of the metastable smectic form to the highly stable monoclinic form as the annealing temperature is increased, resulting in an enhanced degree of crystallinity and the crystallite size. The improvements in the degree of crystallinity and the crystallite size became more remarkable above 120°C. Evaluation of the crystallinity was carried out using an analysis of density, infrared spectroscopy, and X-ray diffraction methods whereas the state of the molecular orientation was evaluated using polarized infrared spectroscopy measurements only. Polarized infra-red spectroscopy measurements after the curve fitting procedure showed a slight increase of the molecular orientation of the helical chain segments present in the crystalline phase represented by the IR bands at 841 and 998 cm^{-1} whereas the amorphous structure represented by the IR band at 974 cm^{-1} showed no significant change with increasing annealing temperature. The improvement in the molecular orientation of the crystalline phase became more remarkable above 120°C. Tensile strength of the annealed fibers increased with increasing annealing temperature but the elongation at break and the initial modulus were not affected as much as the tensile strength. J Appl Polym Sci 122: 3322–3338, 2011

Key words: isotactic polypropylene fiber; infra-red spectroscopy; X-ray diffraction; density; crystallinity; tacticity

INTRODUCTION

Polypropylene molecules mainly consist of long backbone carbon–carbon chain structure incorporating methyl (CH_3) groups attached from the side of the main chain leading to different tacticities (i.e., isotactic, syndiotactic, and atactic). In isotactic polypropylene, methyl groups are arranged along the same side, whereas in the syndiotactic polypropylene alternating methyl groups are arranged on the opposite sides of the polymer chain. Because of the regular, repeating arrangement, isotactic polypropylene tends to have a high degree of crystallinity. In the case of atactic polypropylene, methyl groups are arranged randomly on both sides of the polymer chain.

The tacticity is known to have an important effect on the properties of the polymer. Isotactic and syndiotactic polypropylene result in the formation of regular crystalline structures which enable the polymer chains to pack efficiently. As far as the commercial aspects are concerned, 90% of the polypropylene resin is produced in isotactic form due to its desirable fiber forming characteristics, low density and mechanical properties.

The structures of polypropylene are generally classified into crystalline, mesophase also known as paracrystalline or smectic and amorphous phases. Polymorphism in isotactic polypropylene is well documented in the literature.[1–3]

In the crystalline structures, the polymer chains are characterized by the presence of helical conformations and the differences in crystal structures are mainly due to the relative positioning and the mutual registration of the helical chains with respect to each other. The vast amount of published literature points to the presence of at least three crystalline structures, namely α, β, and γ forms. The α-form is readily obtained and is the most stable and well documented in the published literature.[2,4,5] The α-form assumes monoclinic crystal structure and the

Correspondence to: I. Karacan (ismailkaracan@erciyes.edu.tr).

Contract grant sponsor: Scientific Research Projects Unit of Erciyes University; contract grant number: FBA-09-955.

unit cell contains 12 monomeric units. Each polymer chain is characterized by a 3_1 helical conformation with *c*-axis running parallel to the helix axis. α-phase is usually obtained from slowly crystallized unstrained melt or solution.[4] The formation conditions for the β and γ phases are reported to be dependent on molecular weight, the degree of isotacticity, and the thermal treatment of the sample.[1] The β-hexagonal phase first reported by Keith et al.[5] is reported to form hexagonal crystalline structure under specific conditions being less stable than the α-form.

β-hexagonal phase is formed by the crystallization from the melt with operation temperatures ranging from 100 to 130°C,[2] nonisothermal crystallization of compression molded melt under controlled pressure[6] and the crystallization from the melt in the presence of nucleating agents, such as pimelic acid and calcium stearate[7] or calcium dicarboxylates.[8] The preparation of 100% pure β-hexagonal phase polymer is reported by Li et al.[9]

In the unit cell of hexagonal phase, the helices are located in alternative rows with opposite direction and they possess the same sense of rotation. The axial repeat distance of hexagonal phase is found to be slightly less ($c = 0.635$ nm)[5] than that found in the monoclinic cell ($c = 0.650$ nm).[4] The β-hexagonal phase is found to transform itself to more stable α-phase upon heat treatment or annealing.[2,5] From the point of view of industrial applications, it is important to have high fraction of β-hexagonal phase which is reported to improve the toughness of isotactic polypropylene.[10,11]

The γ-phase was first observed by Addink and Beintema[1] in 1961 and its crystal structure was identified as triclinic by Morrow and Newman[12] which was believed to be similar to that of the α-phase. The formation of γ-phase can be achieved by suitable crystallization of stereoblock fraction of isotactic polypropylene,[2] using low molecular weight isotactic polypropylene[1,12] and crystallization of the polymer under elevated pressure,[13,14] or atmospheric pressure.[15,16]

The formation of γ-phase seems to be preferred in the presence of structural defects in the isotactic polypropylene chain.[17] Meille et al.[18] refined the orthorhombic unit cell of γ-phase using the X-ray diffraction data collected at −120°C which led to a new proposal of crystal architecture with nonparallel chain axes. The unit cell is reported to be formed by bilayers composed of two parallel helices, and the direction of nonparallel chain axis in adjacent layers being tilted at an angle of 80°.

Isotactic polypropylene is known to crystallize into a variety of crystal modifications by slowly cooling the melt.[2,4,5] However, rapid quenching from the melt below 0°C with a cooling rate higher than 80°C/s[19] produces a phase of low structural order described as a glass or mesomorphic state which has been the subject of various investigations in the past.[4,19–25] Natta and Corradini[4] pointed out that the mesomorphic phase possesses an intermediate degree of order between the amorphous phase and the crystalline phase. They referred to this structure as "smectic" form to indicate the presence of two-dimensional order which essentially consists of three-fold helical conformation usually found in the α-monoclinic crystalline phase but consists of a disorder in the packing of the polymer chains perpendicular to their axes.

It was suggested[4,26] that the mesophase consists of pseudohexagonal structure in which right and left-handed helices of molecular structure are placed at random with respect to each other. In an alternative study, Miller[20] and Fujijama et al.[21] put forward an alternative proposal that the quenched form of isotactic polypropylene could be described as a paracrystal of the type suggested by Hosemann.[27]

Another alternative proposal is provided by Gailey and Ralston[22] and Murthy et al.[23] who suggested that the quenched form consisted of micro-crystallites of the hexagonal phase of isotactic polypropylene. The formation of nano-crystallites from the quenched form has been proposed by Ferrero et al.[24] Micro-crystallite dimensions are reported to be between 5 and 10 nm for the hexagonal β-phase structure[22] and 3 nm for the cubic or tetragonal phase structure.[25]

Corradini et al.[28,29] compared the measured X-ray diffraction intensities with those calculated scattering data based on the Fourier transform analysis and presented the results suggesting the impossibility of the formation of micro-crystallites from either α-monoclinic or β-hexagonal structures. Wunderlich et al.[30] suggested that confirmationally disordered crystal definition would be more appropriate for the mesomorphic form of isotactic polypropylene.

The existence of the mesomorphic form was also reported during the melt-spinning of isotactic polypropylene fibers as well.[31–33] Sheehan and Cole[31] in the early 1960s showed that α-monoclinic polypropylene is produced under normal air solidification, whereas solidification in cold water is reported to prevent crystallization and results in a highly oriented but poorly ordered paracrystalline structure, which was later referred to as mesomorphic phase meaning the phase between the amorphous and crystalline phase. In an investigation carried out by Tomka et al.,[32,33] it was confirmed that as-spun paracrystalline fibers of low orientation can be considered to be the best precursors for achieving high strength after a suitable drawing stage. In a further study[33] they showed the effects of heat-treatment, one-stage and two-stage drawing on the structure

TABLE I
Details of Fiber Production Parameters

Process parameters		Comments
MFI		25 g/10 min
Extrusion temperature		235°C ± 2°C
Take-up speed		2500 m min^{-1}
Cooling unit temperature		18–19°C
Air blow speed		40–70 m s^{-1}
Spinnerette pressure		60–70 bar
Spinnerette hole number		72
Spinnerette hole diameter (R)		200–400 μm
Hole shape		Δ (Trilobal)
Throughput		9.12 g min^{-1}
Yarn tension (for 300 denier)		32–33 cN
Environmental conditions	Relative humidity	70%
	Temperature	15°C

and properties of the final as-spun fibers. This study showed the effect of increasing the orientation of paracrystalline phase followed by converting this structure to a more stable α-monoclinic phase.

The aim of the present study is to investigate the fiber structure development and establish the structure–property relationships of isotactic polypropylene fibers annealed at temperatures ranging from 60 to 140°C. In addition, structural charaterization was carried out using combination of density, infrared spectroscopy, X-ray diffraction, and mechanical property measurements.

EXPERIMENTAL

Fiber production

The melt-spun as-spun isotactic polypropylene fibers were produced using Barmag® CF melt-spinning machine operating at an extrusion speed of 2500 m min^{-1}. Fiber production details are presented in Table I. Extrusion temperature was set at 235°C ± 2°C. Fiber grade polypropylene granules with weight average molecular weight of 179,000 and polydispersity (M_w/M_n) of 4.6 obtained from Basell Polyolefins with a nominal MFI of 25 g/10 min were used during the fiber extrusion stages. Melt-Flow Index measurements were carried out according to ASTM D1238 using a load for extrusion of 2.16 kg. The melt-extruded filaments were immediately solidified with the assistance of cooling air with a blow speed of 40–70 m s^{-1} and a cooling air blow temperature of 18–19°C. During the melt-extrusion stage, a spinnerrette pressure of 60–70 bar and spinnerrette hole diameter of 200–400 μm was utilized. The filaments had a trilobal cross-sectional shape with a smooth surface as shown in Figure 1. The melt-extrusion was performed with environmental conditions having the typical characteristics of 70% relative humidity and 15°C air temperature.

The samples were wound onto stainless steel frame with the aim of constraining the samples under constant length to prevent the physical shrinkage and also to prevent the loss of molecular orientation. Annealing was performed in an air heated environment at a temperature range of 60–140°C with 10°C increments for 45 min. During the annealing stage, a heating rate of 1°C min^{-1} was utilized.

EXPERIMENTAL DATA COLLECTION

X-ray diffraction

Equatorial X-ray diffraction traces were obtained using a Bruker® AXS D8 Advance X-ray diffractometer system utilizing nickel filtered Cu Kα radiation (wavelength of 0.154056 nm) and voltage and current settings of 40 kV and 40 mA, respectively. Counting was carried out at 10 steps per degree. The observed equatorial X-ray scattering data was collected in the 10°–35° 2θ range.

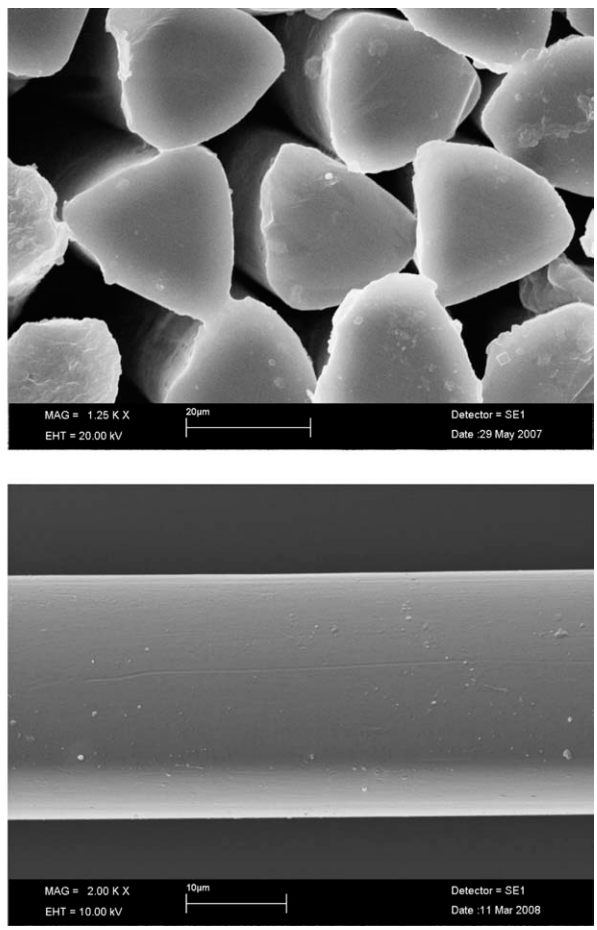

Figure 1 SEM images of isotactic polypropylene fiber extruded at an extrusion speed of 2500 m min^{-1}. (a) cross-sectional view; (b) lateral view.

Infra-red spectroscopy measurements

Perkin–Elmer® Spectrum 400 FT-IR spectrometer was employed for infrared measurements using single reflection diamond crystal based GladiATR® model ATR attachment. ATR-IR technique is known to be a surface characterization technique and is known to be sensitive to about a few microns into the surface of the samples. In some cases depth of beam penetration can be as much as 1.66 μm at 1000 cm^{-1} for diamond ATR crystals and 0.65 μm at 1000 cm^{-1} for germenium ATR crystals. All the spectra were collected in the mid-IR range (i.e., 4000–400 cm^{-1}) with co-added 50 scans collected at a resolution of 2 cm^{-1}. Finally, all the spectra were analyzed using the OMNIC software® and curve fitting procedures to obtain accurate peak parameters.

Density measurements

Density values were evaluated using a density gradient column operating at 23°C. The column was prepared using isopropyl alcohol ($\rho = 0.785$ g cm^{-3}) and water for the measurement of the density of the as-spun filaments. The samples were allowed $\sim$ 24 h to reach their equilibrium level of displacement. The fractional crystallinity (χ_c) values of the samples were then estimated using the Eq. (1).

$$\chi_C = \frac{\rho_C(\rho - \rho_a)}{\rho(\rho_c - \rho_a)} \times 100 \quad (1)$$

where ρ_c and ρ_a are the densities of crystalline and amorphous polypropylene. Fractional crystallinity was evaluated from the densities using the crystalline and amorphous densities as 0.936[4,34] and 0.850[34,35] g cm^{-3}, respectively.

Mechanical property measurements

Mechanical properties were measured using Zwick-Roell 1446 tensile tester at room temperature. A crosshead speed of 12.5 mm min^{-1} was used for all experiments. The initial length of the sample was set at 25 mm. Careful attention was taken to minimize stretching and slippage of the filaments before testing while placing the sample in the grips. Tensile modulus was evaluated from the initial slope of the tensile curve. The elongation and tensile strength at break were determined at the position of break. Tensile strength and tensile modulus were calculated in textile units of GPa. Reported values were averages of at least 20 tests.

EXPERIMENTAL DATA ANALYSIS

X-ray data-curve fitting

All the X-ray diffraction traces obtained from the annealed isotactic polypropylene samples were fitted with a curve fitting procedure developed by Hindeleh et al.[36] to separate overlapping peaks. Each profile is considered to have the combination of Gaussian and Cauchy functions. When the observed and calculated intensity traces converge to the best acceptable parameters, the computer program provides the list of accurate peak parameters in terms of profile function parameter (*f*), peak height, half-height width and peak position. When the profile function parameter (*f*) is equal to unity gives a Gaussian intensity distribution and when equal to zero gives a Cauchy shape. Initially, a value of (*f*) equal to 0.5 is given to start the fitting process and then the minimization procedure finds the best peak parameters.

Evaluation of the apparent X-ray crystallinity

Apparent X-ray crystallinity is based on the ratio of the integrated intensity under the resolved peaks to the integrated intensity of the total scatter under the experimental trace.[37] This definition can be expressed as in the Eq. (2)

$$\chi_c = \frac{\int_0^\infty I_{cr}(2\theta)d(2\theta)}{\int_0^\infty I_{tot}(2\theta)d(2\theta)} \quad (2)$$

The area under the background is considered to correspond to the noncrystalline scatter (i.e., amorphous phase). It should be emphasized that the apparent X-ray crystallinity is defined between two arbitrarily chosen angles and should be considered an optimum mathematical solution. In this work, the apparent X-ray crystallinity was estimated in the 2θ range between 10° and 35°.

Evaluation of the apparent crystallite size

The peak widths at half-height have been corrected using the Stoke's deconvolution procedure.[38] Finally, the apparent crystallite size of a given reflection was calculated using the Scherrer equation:

$$L(hkl) = \frac{K.\lambda}{\beta.\cos(\theta)} \quad (3)$$

where θ is the Bragg angle for the reflection concerned, λ is the wavelength of radiation (wavelength of 0.154056 nm), *L*(hkl) is the mean length of the crystallite perpendicular to the planes (hkl), β is either the integral breadth or the breadth at half maximum intensity in radians, and *K* is a Scherrer parameter usually taken as 1 for integral breadths and 0.89 for half-widths. Hexamethylene-tetramine compacted at 85°C was used for the instrumental broadening correction.

Infra-red spectroscopy data-curve fitting

In the present work the parallel and perpendicular polarization spectra were fitted independently, allowing the peak positions and half-height widths to vary freely, using the peak positions previously found using OMNIC® software as a guide to the starting values. Finally, the peak positions and the half-height widths obtained from the two spectra were averaged and the parallel and perpendicular spectra were refitted, fixing the positions and the half-height widths at these average values and allowing only the peak heights to vary.

The infra-red spectrum of isotactic polypropylene in the 1025–775 cm^{-1} region contains at least six well-defined peaks located at 809, 841, 899, 940, 973, and 998 cm^{-1}. During the curve fitting stages it was necessary to include additional peaks at 796, 827, 852, 886, 931, and 955 cm^{-1} to improve the fits in the tail regions of the major peaks. In the second stage, the IR peak located at 973 cm^{-1} is split into two peaks one at 972 cm^{-1} and the other at 974 cm^{-1}. Curve fitting was restricted to 923–1025 cm^{-1} region for the second stage. Additional peaks needed to improve the fitting are located at 931, 950, 955, and 966 cm^{-1}, respectively. All the IR spectra obtained from the annealed isotactic polypropylene fiber samples were fitted with a curve fitting procedure developed by Hindeleh et al.[36] to separate overlapping peaks.

Evaluation of tacticity

The isotacticity has been measured by means of the absorbance ratios of the IR bands at 841, 973, and 998 cm^{-1} using the absorbance values obtained during the curve fitting stages. 973 cm^{-1} band has been used as an internal standard due to its presence in the IR spectrum of melted polymer.[39] The absorbance ratios examined in the present investigation are: A_{998}/A_{973} and A_{841}/A_{973}. Assuming the absence of syndiotactic propylene sequences in the polymer chain, the tacticity is calculated as the sum of the fraction of isotactic and atactic propylene sequences, hence atacticity is calculated using the Eq. (4)

$$\chi_{\text{atacticity}} = 1 - \chi_{\text{isotacticity}} \tag{4}$$

Evaluation of crystallinity

Certain infra-red bands tend to show absorbance increases following either orientation due to high extrusion speeds, through drawing processes or during annealing stages. The crystalline fraction in the crystalline phase is calculated using the Eq. (5).

$$\chi_{\text{crystalline}} = \frac{\sum A_{\text{crystalline}}}{\sum A_{\text{crystalline}} + \sum A_{\text{amorphous}}} \tag{5}$$

where $\Sigma A_{\text{crystalline}} = A_{998} + A_{899} + A_{841} + A_{809}$ and $\Sigma A_{\text{amorphous}} = A_{974,}$ respectively. Since the sum of the crystalline content and the amorphous content must be equal to unity, the amorphous fraction is evaluated by the Eq. (6).

$$\chi_{\text{amorphous}} = 1 - \chi_{\text{crystalline}} \tag{6}$$

Calculation of the orientation parameters of polarized infra-red data

Because of the uniaxial orientation nature of fibers arising from cylindrical symmetry, the calculation of orientation parameters obtained from the infra-red data analysis can be carried out using the dichroic ratio defined in the Eq. (7)[40]:

$$D = A_{\parallel}/A_{\perp} \tag{7}$$

where $A_{\parallel}$ and $A_{\perp}$ are the measured absorbance values for radiation polarized parallel and perpendicular to the fiber axis, respectively. In this work it is assumed that the polypropylene chains have no preferred orientation around their own axis. The $<P_2(\cos)>$ is known as the second-order Legendre polynomial and is also known as the Herman's orientation factor in the polymer and fiber science. To a good approximation, the dichroic ratio is related to the orientation parameter, $<P_2(\cos\theta)>$, by

$$< P_{200} >=< P_2(\cos\theta) >= \frac{D-1}{D+2}.\frac{2}{(3.\cos^2\alpha - 1)} \tag{8}$$

where θ is the angle between the local chain axis and the fiber axis, and α is the transition moment angle between the associated vibrational mode and the chain axis. $<P_{200}>$ is unity when the polymer chains are parallel to the fiber axis, equal to -0.5 if the polymer chains are aligned perpendicular to the fiber axis and 0 if the polymer chains are distributed randomly.

RESULTS AND DISCUSSION

Thermal treatment, heat setting or more commonly known as annealing procedure is utilized in the treatment of thermoplastic polymers in the form of fibers, uniaxially or biaxially oriented films and injection molded articles. The annealing process permits easier rearrangement of polymer chains depending on the temperature used and for this reason drawing thermoplastic polymers followed by an annealing is often used to enhance the drawing performance. Annealing conditions are known to be heavily dependent on the temperature, duration and environmental conditions used during the processing stages.

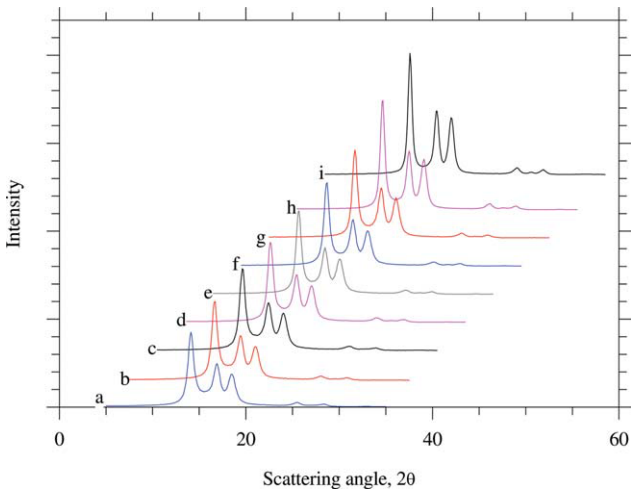

Figure 2 Equatorial X-ray diffraction traces of isotactic polypropylene fibers extruded at an extrusion speed of 2500 m min^{-1} and annealed at (a) 60°C, 45 min; (b) 70°C, 45 min; (c) 80°C, 45 min; (d) 90°C, 45 min; (e) 100°C, 45 min; (f) 110°C, 45 min; (g) 120°C, 45 min; (h) 130°C, 45 min; (i) 140°C, 45 min. [Color figure can be viewed in the online issue, which is available at wileyonlinelibrary.com.]

Annealing carried out under proper conditions is known to enhance the degree of crystallinity and molecular orientation of semicrystalline thermoplastic polymers which in turn directly affect the physical and mechanical properties. For example, increased crystallinity and orientation results in enhanced mechanical properties. Characterization of crystallinity is usually carried out using density,[41] enthalpy of fusion through DSC,[42] X-ray diffraction, NMR, and vibrational spectroscopy (infra-red[43] and Raman[44] techniques), whereas the orientation is usually characterized using polarized infrared[45] and Raman spectroscopy,[46] X-ray diffraction[45] and optical birefringence measurements.[47] These methods provide information at different levels, with their own limitations and advantages. For example, the use of optical birefringence provides an average molecular orientation of crystalline and amorphous phase in terms of the second order orientation averages, whereas X-ray diffraction is only accessible to paracrystalline and crystalline phases and can not detect the presence of totally disordered amorphous phase. However, the use of infrared spectroscopy provides the molecular orientation averages of both crystalline and amorphous phases, respectively.

In the present investigation X-ray diffraction, infrared spectroscopy and density measurements are utilized for the evaluation of the crystallinity whereas the evaluation of molecular orientation is carried out using polarized infrared spectroscopy only. Apparent crystallite size calculations are obtained from the peak parameters of the curve fitted equatorial X-ray diffraction profiles.

X-ray diffraction measurements

Because of the occurrence of polymorphism in the structure of isotactic polypropylene, various annealing conditions were reported to see their influence on the molecular structure.[48,49] Zanetti et al.[48] reported that at a given annealing temperature, half-height widths of the X-ray diffraction reflections decrease with increasing time of treatment. This means that the crystallite size or crystallite perfection increases with increasing time up to a certain maximum value. This maximum value is reached earlier when the annealing temperature is increased.

A close inspection of the equatorial X-ray diffraction traces of annealed as-spun fibers shown in Figure 2 as a function of annealing temperature shows three strong [(110), (040) and (130)], well defined and intense peaks together with two weak reflections [(060) and(220)]. Monoclinic crystalline form appears to have α_1 and α_2 forms. Both α_1 and α_2 crystalline forms apparently exhibit identical X-ray diffraction patterns. The X-ray diffraction reflections of the annealed fibers of this investigation show $(h + k)$, an even number revealing the presence of only α_1 crystalline form whereas α_2 crystalline form exhibits $(h + k)$ odd numbers.[50]

Equatorial X-ray diffraction trace shown in Figure 3 can be fitted with at least six crystalline peaks indexed as 110, 040, 130, 060, 200, and 220, respectively. The indexed peaks corresponds to α-monoclinic phase. During the curve fitting stages, an additional peak located at 15.71° (d-spacing of 0.564 nm) was needed to improve the fit in the tail regions of the neighboring peaks. This peak is relatively broad in half-height width and shows the typical characteristics of a paracrystalline structure.[20,21,31–33]

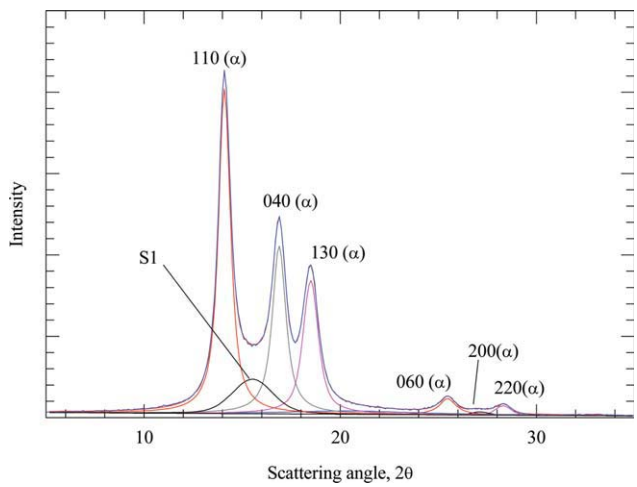

Figure 3 Curve fitting of equatorial X-ray diffraction trace of isotactic polypropylene fiber extruded at a take-up speed of 2500 m min^{-1} and annealed at 60°C for 45 min. [Color figure can be viewed in the online issue, which is available at wileyonlinelibrary.com.]

TABLE II
Peak Parameters of Curve Fitted Equatorial X-Ray Diffraction Trace of Isotactic Polypropylene Fiber Extruded at a Take-Up Speed of 2500 m min^{-1} and Annealed at 60°C for 45 min

Peak ref.	*f*	*A* (height)	HHW (width)	Position (2θ)	*d*-obs spacing (nm)	*d*-calc spacing (nm)
α-110	0.29	1996	0.77	14.13	0.626	0.626
S-1	0.80.	212	2.8	15.71	0.564	–
α-040	0.15	1032	0.87	16.95	0.523	0.522
α-130	0.36	820	1.01	18.55	0.478	0.478
α-060	0.00	100	1.00	25.54	0.348	0.348
α-200	1.00	19	1.21	27.12	0.328	0.328
α-220	1.00	57	1.12	28.40	0.314	0.313

HHW: half-height width; f: profile function parameter.

In the published literature, paracrystalline phase was referred to as smectic phase[7,26] and also as mesophase.[19,24,28,29] The mesophase or smectic phase is known to have an intermediate order between the crystalline and the amorphous phase. It is known that the smectic phase of isotactic polypropylene is quite stable at room temperature for long periods of time, but transforms to the more stable α-monoclinic phase on heating to temperatures above 60°C.[22,28,48] The smectic phase is also reported to undergo a process of solvent induced crystallization at room temperature in different organic solvents including dichloromethane, cyclohexane, carbon tetrachloride, and chloroform.[51] It has also been noted that the increased polymer-solvent interaction via increased sorption of solvent molecules leads to higher level of crystallization. In the smectic phase, the polymer chains containing propylene units adopt helical conformations and are usually arranged parallel to each other on a local scale with little or no lateral register while exhibiting no long range order.

In the present investigation, the paracrystalline peak in the X-ray diffraction traces will be referred to as "smectic" peak being the most preferred name given historically and is identified as S1 in Figure 3.

Curve fitting is a useful procedure to obtain accurate peak parameters. In particular, peak positions provide the values of *d*-spacing which play an important role in the evaluation of unit cell parameters and in the determination of the density of crystalline phase. Peak parameters obtained from the curve fitting procedure together with the observed and calculated *d*-spacing for the sample extruded at a take-up speed of 2500 m min^{-1} and annealed at 60°C for 45 min are compared in Table II.

X-ray diffraction patterns of isotactic polypropylene produced from rapidly quenched melt containing smectic phase is reported to contain two broad halos with *d*-spacing of 0.564 nm ($2\theta = 15.71°$) and 0.4 nm ($2\theta = 22°$), respectively. The peak located at 15.7° is related to the interatomic vector between adjacent chains in the smectic phase and is not related to the stereoregularity (or tacticity) of the polymer chains.[52]

The 2nd smectic peak with a *d*-spacing of 0.4 nm seems to disappear from the equatorial X-ray diffraction traces and move to the first layer line when a highly oriented and drawn sample is produced.[53] This is the reason why only one peak at $2\theta = 15.7°$ was used in the curve fitting of the equatorial X-ray diffraction traces of the highly oriented and annealed fiber samples under investigation. Close examination of the peak resolution shown in Figure 3 confirms that there in no need to add an additional peak due to the insufficient scattering area under the trace.

Equatorial X-ray diffraction data

The definition of crystallinity can be based on the relative proportion of ordered phase which may exist in a material and is usually evaluated by X-ray diffraction methods. Because of the high sensitivity of X-ray diffraction method to highly ordered regions, it is usually more reliable than the other methods of measuring crystallinity. X-ray crystallinity values evaluated through the use of equatorial diffraction traces via the peak separation procedure can be viewed as a measure of lateral order. Hence, the term "the apparent crystallinity" may be more appropriate to use instead of the "crystallinity" implying absolute crystallinity.

The results obtained from the curve fitting of equatorial X-ray diffraction traces of annealed as-spun fibers suggest that there exists an unambigious structural transformation taking place from a less stable smectic phase to a more stable α-monoclinic phase as the temperature is increased.

X-ray diffraction analysis did not reveal any significant differences between the unannealed original as-spun fibers and the annealed as-spun fibers at a temperature of 60°C. It is highly likely that this temperature is not sufficient enough for the structural transformation to take place. However, significant structural transformation has taken place at annealing temperatures above 70°C as indicated by the significant increases in the intensities of the major

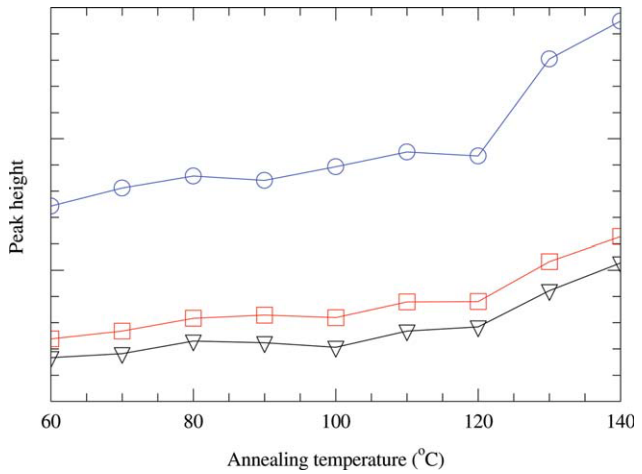

Figure 4 Variation of the peak heights of the equatorial reflections obtained from the X-ray diffraction traces of the annealed as-spun isotactic polypropylene fibers as a function of annealing temperature. 110 (○); 040 (□), and 130 (▽) reflection. [Color figure can be viewed in the online issue, which is available at wileyonlinelibrary.com.]

equatorial reflections (110, 040, and 130) as shown in Figure 4. Peak heights corresponding to the,(110), (040), and (120) reflections show a remarkable steep rise after the annealing temperature of 120°C indicating an enhanced crystallinity and the presence of considerably grown crystallites present in the structure at and above this temperature.

Increases in the intensities of the equatorial reflections are accompanied by narrowing of the half-height widths indicating improved crystallite size and crystallinity. Monoclinic crystalline structure is already formed with the original and unannealed as-spun fiber. Annealing at temperatures higher than 70°C is found to enhance the degree of crystallinity at the expense of smectic phase structure.

Equatorial X-ray diffraction traces presented in Figure 2 reveal that the crystallites are larger as indicated by the narrowing of the peak breadths at half height and more perfect with increasing annealing temperature.

The apparent X-ray crystallinity values evaluated using the Eq. (2) are shown in Figure 5(a). Apparent crystallinity values due to α-monoclinic phase increase continously with increasing annealing temperature and varies between 75 and 88.5%, whereas the smectic phase fraction decreases even below amorphous phase fraction after the annealing temperature of 90°C and is found to range from 12.5 and 3% between 60 and 140°C. It shows that the smectic phase is not completely transformed into the α-monoclinic phase.

It is clear that the structure is composed of a polymorphic structure with main constituents as being α-monoclinic phase together with smectic and unoriented and totally disordered amorphous phase. Amorphous phase fraction is found to vary between 8 and 11%. It seems that the thermally activated transition requires very little molecular realignment to induce the transformation from smectic form to monoclinic form as the movement of the molecular chains are severely restricted in the solid state.[52]

Evaluation of the apparent crystallite sizes

Apparent crystallite size calculations usually take into account the broadening imposed by the finite width of the X-ray diffractometer beam. This behavior is reflected as a broadening of the peak width and must be corrected using an appropriate procedure. In the present investigation, the correction of the half-height widths are carried out according to the Stoke's deconvolution method.[38]

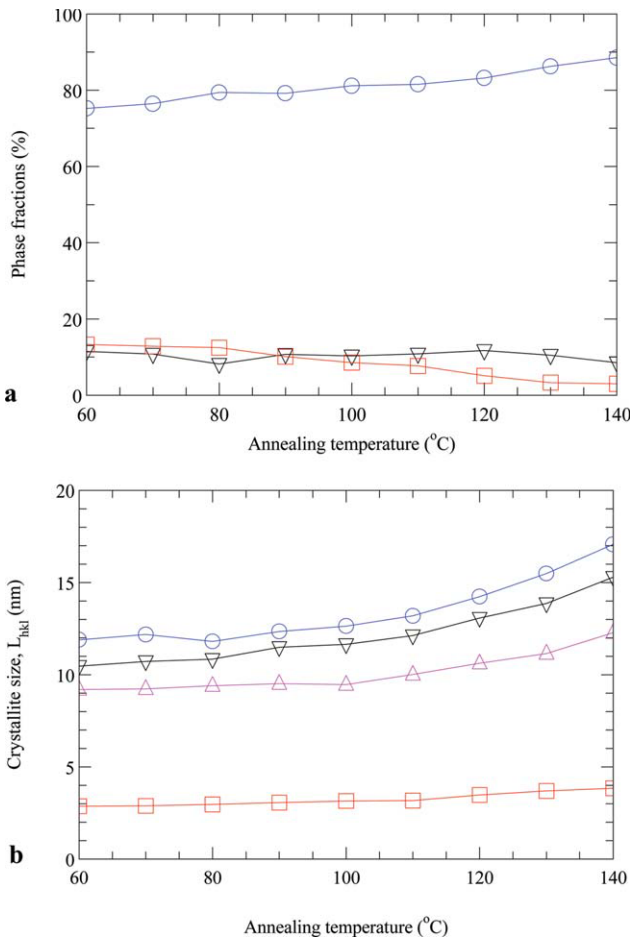

Figure 5 (a) Comparison of α, smectic and amorphous phase fractions obtained from X-ray diffraction for the annealed isotactic polypropylene fibers as a function of annealing temperature. (○) α-phase, (□) smectic phase, and (▯) amorphous phase. (b) Comparison of the crystallite size of the annealed isotactic polypropylene fibers as a function of annealing temperature. (○) 110; (▯) 040; (△) 130; and (□) smectic peak. [Color figure can be viewed in the online issue, which is available at wileyonlinelibrary.com.]

Once the observed half-height widths are corrected for the instrumental effects, then the corrected half-height widths can be used in the crystallite size calculations. For this reason, Scherrer's Eq. (3) is used for the determination of the crystallite sizes arising from the presence of α-monoclinic and smectic forms.

α (110) peak parameters

This is the narrowest peak in the equatorial X-ray diffraction trace which gives the highest crystallite size in comparison with the other peaks. Corrected half-height widths of the (110) peak due to the α-monoclinic phase shows gradual decrease from 0.57 to 0.52°. Crystallite sizes perpendicular to the (110) planes following the half-height-width correction show an increase from 12 to 17 nm [Fig. 5(b)] corresponding to an increase from 19 to 28 chains in the direction of the planes responsible for the formation of this reflection. It shows that the (110) planes exhibited a net lateral growth of almost 41.7% due to the direct result of the annealing process.

α (040) peak parameters

Corrected half-height widths of the (040) peak due to the α-monoclinic phase also show gradual decrease from 0.84 to 0.58°. Crystallite sizes perpendicular to the (040) planes following the half-height-width correction show an increase from 10.5 to 15.3 nm [Fig. 5(b)] corresponding to an increase from 20 to 29 chains in the direction of the planes responsible for the formation of this reflection. It shows that the (040) planes exhibited a net lateral growth of almost 45% due to the direct result of the annealing process. It shows that the crystallite size grows more in the (040) planes direction than that of the (110) planes.

α (130) peak parameters

Corrected half-height widths of the (130) peak due to the α-monoclinic phase show gradual decrease from 0.97° to 0.73°. Crystallite sizes perpendicular to the (130) planes following the half-height-width correction shows an increase from 9.2 to 12.3 nm [Fig. 5(b)] corresponding to an increase from 19 to 26 chains in the direction of the planes responsible for the formation of this reflection. It shows that the (130) planes exhibited a net lateral growth of almost 34% due to the direct result of the annealing process. It shows that the crystallite size growth of the (130) planes is slightly less than that of the (110) and (040) planes, respectively.

Smectic phase peak parameters

Corrected half-height widths of the S1 peak due to the smectic phase show gradual decrease from 3.12° to 2.33°. Crystallite sizes for this peak following the half-height-width correction show an increase from 2.9 to 3.8 nm [Fig. 5(b)] corresponding to an increase from 5 to 7 chains in the direction of the planes responsible for the formation of this reflection. It shows that the smectic S1 planes do not exhibit much growth due to the transformation to α-monoclinic phase.

Infrared spectroscopy results

Tacticity measurements

The ability to form regular helices depends on the degree of isotacticity which can be estimated directly by determining the amount of insoluble residue remaining after extraction with boiling *n*-heptane and other organic solvents such as acetone and diethyl ether.[41] The solvent extraction method involves extracting soluble atactic fraction after boiling isotactic polypropylene in *n*-heptane where the remaining matter is insoluble isotactic polypropylene. This method is believed to be expensive, time consuming and is subject to errors. For these reasons, relatively simple, rapid, accurate and easy to use method of IR spectroscopy is used in the present investigation.

The isotacticity has been measured by means of the absorbance ratios of the IR bands at 998, 973, and 841 cm^{-1}, A_{998}/A_{973} and A_{841}/A_{973}, using the absorbance values obtained during the curve fitting stages (Table V). The 998 cm^{-1} band is assigned to CH_3 rocking + CH_2 wagging + CH bending vibrations, whereas the 973 cm^{-1} band belongs to strongly coupled CH_3 rocking + C—C chain stretch vibrations. The 841 cm^{-1} is assigned to CH_2 rocking + C—CH_3 stretching (Table III).

Assignments of the IR bands in the 1400–800 cm^{-1} region is presented in Table III.[54] 998 and 841 cm^{-1} absorption bands are found to correspond to the crystalline phase,[55] whereas 973 cm^{-1} band contains contributions from the crystalline and the amorphous phases. 973 cm^{-1} band is associated with the presence of short isotactic helices apparently present in the melt or in the atactic material.[39,55] This peak has been attributed to the superposition of two peaks, the IR peak located at 972 cm^{-1} is assigned to the crystalline phase whereas the other IR peak located at 974 cm^{-1} is assigned to the amorphous phase.[45] It appears that the amorphous phase still contains a certain amount of helical polymer chain segments. The height of the band at 973 cm^{-1} is found to be essentially insensitive to the structural changes due to the crystallization effects. The bands

TABLE III
Assignment of Polypropylene Infrared Absorption Bands in the 1400–800 cm^{-1} Spectral Region

Frequency (cm^{-1})	Phase	Polarization	Assignment[54]
1377	A,C	⊥	CH_3 symmetric bending + CH_2 wagging
1256	A,C	∥	CH bending + CH_2 twisting + CH_3 rocking
1220	C	⊥	CH_2 twisting + CH bending + C—C chain stretching
1168	C	∥	C-C chain stretching + CH_3 rocking + CH bending
1104	C	⊥	C-C chain stretching + CH_3 rocking + CH_2 wagging + CH twisting + CH bending
1044	C	∥	C-CH_3 stretching+C—C chain stretching + C—H bending
998	C	∥	CH_3 rocking+CH_2 wagging + CH bending
973	A,C	∥	CH_3 rocking + C—C chain stretch
941	C	⊥	CH_3 rocking + C—C chain stretch
900	C	⊥	CH_3 rocking + CH_2 rocking + CH bending
841	C	∥	CH_2 rocking + C—CH_3 stretching
809	C	⊥	CH_2 rocking + C—C stretching + C—H stretching

C = crystalline, A = amorphous.

normally used for the tacticity measurements are usually found to disappear upon melting.[56]

Tacticity measurements are performed after obtaining the absorbance values of the relevant IR bands using curve fitting procedure. Curve fitting is performed in the 1025–775 cm^{-1} region, a typical curve fitting of this region is shown in Figure 6 together with the listing of the peak parameters in Table IV for the sample annealed at 60°C for 45 min. The isotacticity values are evaluated using the absorbance ratios of A_{998}/A_{973}, A_{841}/A_{973} and atacticity values are evaluated using the Eq. (2). The results are presented in Table V and Figure 7.

The results presented in Figure 7 show that the isotacticity fractions obtained from the absorbance ratio of A_{841}/A_{973} is always higher than that of the absorbance ratio of A_{998}/A_{973} for the samples annealed in the temperature range of 60–140°C. This may be attributed to the absorption band at 998 cm^{-1} being slightly sensitive to less ordered phase.

Zhu et al.[57] reported the existence of the band at 998 cm^{-1} at a temperature of 220°C being at least 60°C above the melting point and showed that a small fraction of ordered helical polymer chain segments still exist in the melt. The IR spectrum of the polypropylene melt indicated that during the melting process not all the helices disappeared. Following the melting, this peak significantly lost its intensity but did not disappear completely. It shows that certain amount of helical chain segments still exist in the molten phase implying some short range order in the melt. The length of these segments is reported to be at least about five propylene units in the melt.[58]

The regularity band at 841 cm^{-1} shows the lowest peak width in comparison with the other helical bands (Table IV). This peak has an average half-height width of 7.7 cm^{-1}. It has also has been

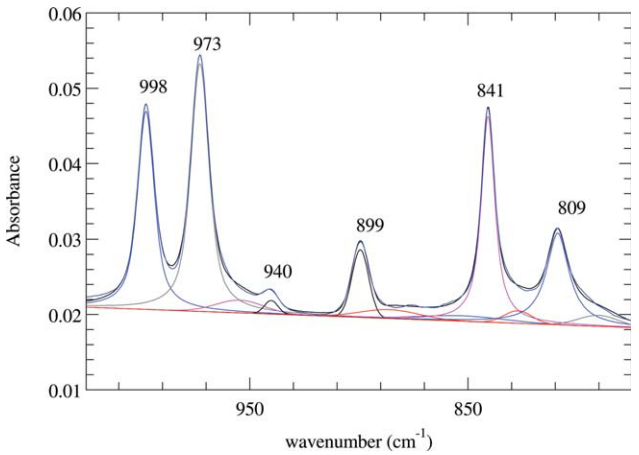

Figure 6 Curve fitting of the infra-red spectrum of isotactic polypropylene fiber extruded at 2500 m min^{-1} and annealed at 60°C for 45 min in the 1025–775 cm^{-1} spectral range. [Color figure can be viewed in the online issue, which is available at wileyonlinelibrary.com.]

TABLE IV
Resolved IR Peak Parameters for Isotactic Polypropylene Fiber Extruded at 2500 m min^{-1} and Annealed at 60°C for 45 min

Peak no.	Profile function parameter	Absorbance (peak height)	Half-height width (cm^{-1})	Peak position (cm^{-1})
1	1.0	0.0014	26.0	790
2	0.0	0.0121	12.5	809
3	1.0	0.0016	17.8	827
4	0.9	0.0273	7.7	841
5	1.0	0.0007	55.5	852
6	1.0	0.0011	38.2	886
7	1.0	0.0090	10.8	899
8	0.0	0.0001	0.2	931
9	1.0	0.0018	8.8	940
10	1.0	0.0017	30.8	954
11	0.4	0.0329	10.9	973
12	0.3	0.0263	9.9	998

1025–775 cm^{-1} range.

TABLE V
% Isotacticity and Atacticity Values of Isotactic Polypropylene Fibers Annealed at 60–140°C

Annealing temp (°C)	A_{998}/A_{973} Isotacticity (%)	A_{998}/A_{973} Atacticity (%)	A_{841}/A_{973} Isotacticity (%)	A_{841}/A_{973} Atacticity (%)
60	79.9	20.1	83.0	17.0
70	80.1	19.9	85.8	14.2
80	80.7	19.3	88.3	11.7
90	80.7	19.3	89.2	10.8
100	81.1	18.9	89.3	10.7
110	81.6	18.4	90.2	9.8
120	82.6	17.4	90.4	9.6
130	83.7	16.3	91.4	8.6
140	85.3	14.7	93.2	6.8

assigned to long helical chains with an average length of 12–14 propylene units.[56] The fraction of isotacticity obtained from the absorption ratio of A_{841}/A_{973} varies between 83 and 93%. Assuming no syndiotactic propylene segments in the polypropylene chains then the atacticity fraction lies in the 17–7% range (Fig. 7). The value of isotacticity fraction tends to show an upward trend after the annealing temperature of 60°C. This may be due to the effect of crystallization and the subsequent increase in the fraction of the highly ordered material.

Evaluation of crystallinity by the infrared and density measurements

During the past few decades, infrared spectroscopy has been extensively utilized in the structural characterization of isotactic polypropylene. Many investigations showed that specific regularity bands are related to the critical length of isotactic sequences. It was found that the absorption intensity of 998 cm^{-1} band disappears as the sequence length becomes less than 10 monomeric units. Crystalline isotactic polypropylene IR regularity bands located at 1220, 1168, 998, 899, 841, and 809 cm^{-1} are defined as helix bands.[56] Kobayashi et al.[59] showed that only 841 and 998 cm^{-1} bands remain for monomeric sequence lengths less than 10 in the IR spectra of isotactic copolymer and deuteropropylene copolymers.

The use of density for the evaluation of fractional crystallinity using the Eq. (1) is well established, although in many cases disputed due to the use of assumption that the structure is composed of only crystaline and amporphous phases only. The values of the density are shown in Table VI and the fractional crystallinity values are listed in Table VI together with the values of the amorphous fractions. The data presented in Table VI exhibit a gradually increasing density and fractional crystallinity values as a function of annealing temperature. It is believed that due to the effects of annealing process, increases in the density and crystallinity are expected to occur in response to increasing annealing temperatures. Figure 8 shows that the infrared absorption band ratios of A_{998}/A_{973} and A_{841}/A_{973} are plotted against the measured density values for the annealed isotactic polypropylene fibers. The linearity of the plots presented in Figure 8 shows that the infrared absorption of the regularity bands at 998 and 841 cm^{-1} and the density depends on the degree of crystallinity in the same direction. The correlation of the absorption ratio of A_{841}/A_{973} with density is more successful than that of the case with the absorption ratio of A_{998}/A_{973}. There exists a similar correlation between the α-phase crystallinity and the measured density values as shown in Figure 9.

To obtain the fraction of amorphous phase and the crystalline phase, curve fitting of the IR spectrum was carried out in two stages. In the first stage, the 1025–775 cm^{-1} spectral region was resolved into separate IR bands at 998, 973, 940, 899, and 841 cm^{-1} as shown in Figure 6. In the second stage, the

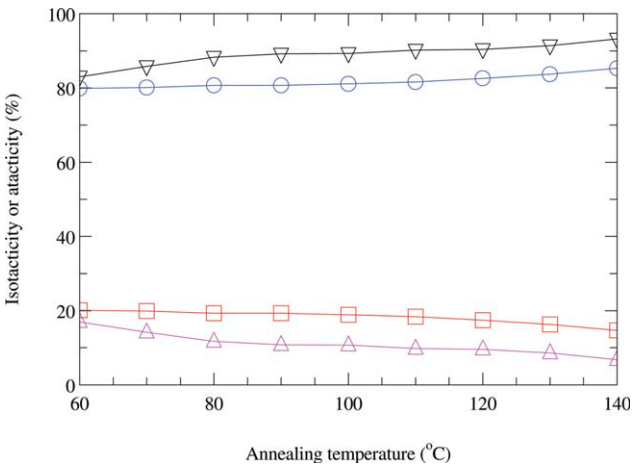

Figure 7 Effect of the annealing temperature on the isotacticity and atacticity of isotactic polypropylene fibers. (▽) A_{841}/A_{973} (%); (○) A_{998}/A_{973} (%); (□) 100- A_{998}/A_{973} (%); (△) 100- A_{841}/A_{973} (%).[Color figure can be viewed in the online issue, which is available at wileyonlinelibrary.com.]

TABLE VI
Characteristics of Isotactic Polypropylene Fibers Annealed Between 60–140°C

Annealing temperature (°C)	Density (g cm^{-3})	Fractional crystallinity (%)	Amorphous fraction (%)
Unannealed	0.8651	19.0	81.0
60	0.8711	26.4	73.6
70	0.8837	41.5	58.5
80	0.8907	49.7	50.3
90	0.9047	65.8	34.2
100	0.9117	73.7	26.3
110	0.9119	73.9	26.1
120	0.9159	78.3	21.7
130	0.9164	78.9	21.1
140	0.9205	83.4	16.6

curve fitting of 1025–923 cm^{-1} spectral region shown in Figure 10 was carried out to obtain the amorphous band parameters by splitting the IR band at 973 cm^{-1} into 972 cm^{-1} as crystalline component and 974 cm^{-1} bands as amorphous component, respectively.

This way the IR crystallinity can be evaluated using the Eq. (5). Crystallinity measurements listed in Table VI and presented in Figure 11 show that the crystallinity values derived from IR spectroscopy are significantly higher than the density derived crystallinity in the annealing temperature range of 60–130°C. The large differences in the crystallinity values may be due to the assumption that the amorphous density used in the evaluation of crystallinity from density measurements remains constant. It is most likely that the amorphous density will increase with increasing annealing temperature. It is also true that the helical segments normally present in the crystalline phase is also most likely to be present in the smectic and amorphous phases. This point partly explains why the crystallinity values obtained from IR-spectroscopy do not show much change during the annealing stages.

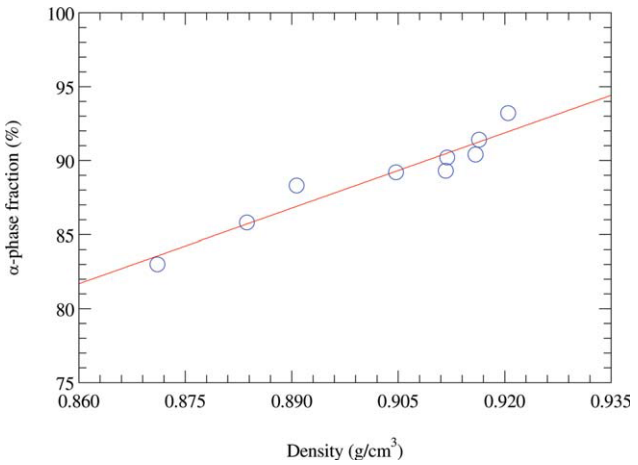

Figure 9 Comparison of the α-monoclinic crystallinity obtained from the X-ray diffraction analysis with the measured density values for the annealed isotactic polypropylene fibers. [Color figure can be viewed in the online issue, which is available at wileyonlinelibrary.com.]

It has been reported that the values of the crystallinity seem to be affected by the molecular weight and the crystallization conditions.[60] The amount of crystallinity and the melting point are reported to be lowered by decreasing crystallization temperature and by increasing molecular weight. At a fixed molecular weight of the polymer, the degree of crystallinity is reported to increase with increasing crystallization temperature due to the effect of lowered crystallization rate as well as the ability of the polymer chains to gain more mobility to be orderly

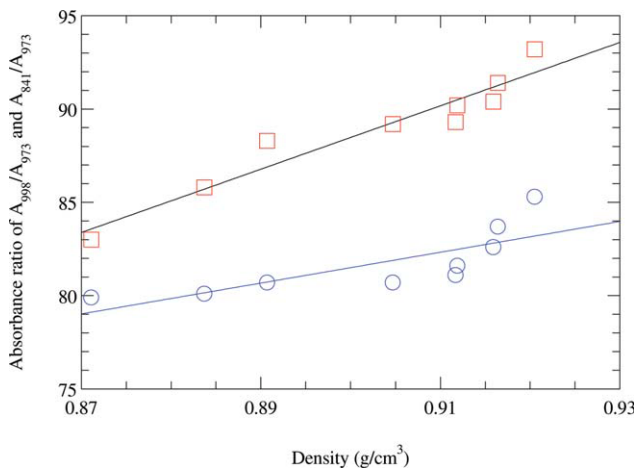

Figure 8 Correlation of the infrared absorption band ratios of A_{998}/A_{973} (○) and A_{841}/A_{973} (□) with the measured density values for the annealed isotactic polypropylene fibers. [Color figure can be viewed in the online issue, which is available at wileyonlinelibrary.com.]

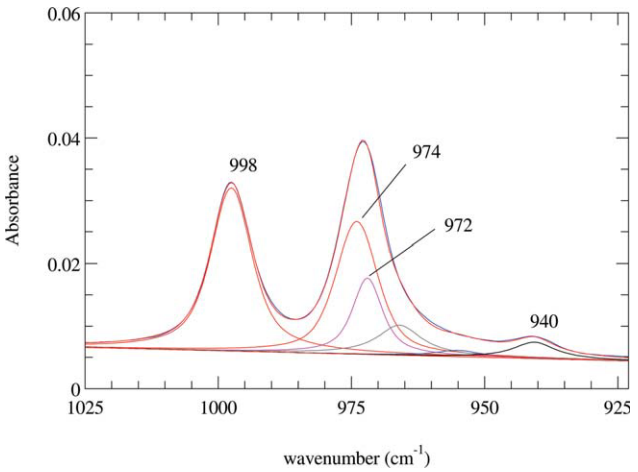

Figure 10 Curve fitting of the infra-red spectrum (1025–923 cm^{-1} range) of isotactic polypropylene fiber extruded at 2500 m min^{-1} and annealed at 60°C for 45 min.[Color figure can be viewed in the online issue, which is available at wileyonlinelibrary.com.]

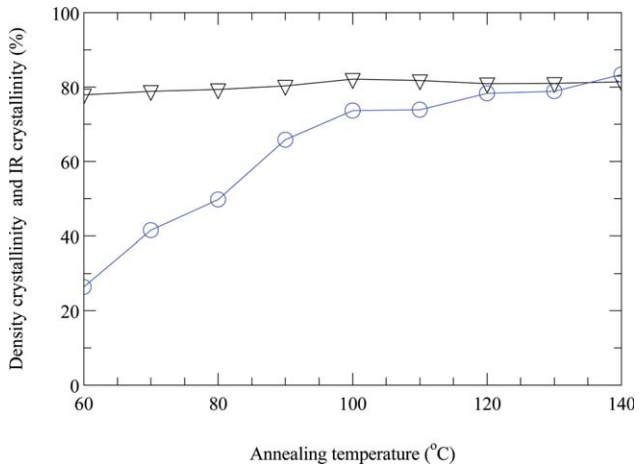

Figure 11 Comparison of the density based crystallinity (○) and the IR crystallinity (▯) of annealed isotactic polypropylene fibers as a function of annealing temperature. [Color figure can be viewed in the online issue, which is available at wileyonlinelibrary.com.]

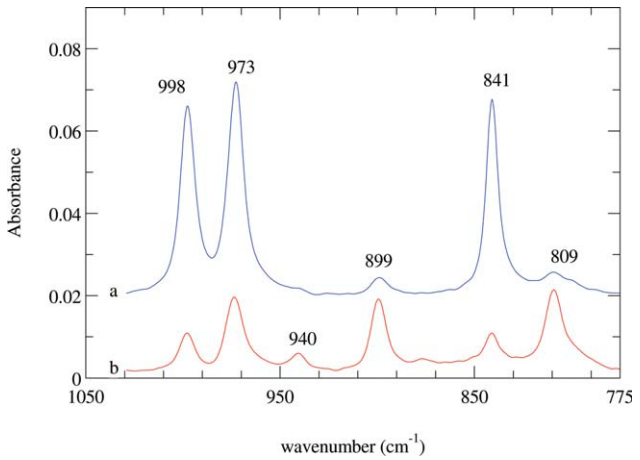

Figure 12 Polarized infrared spectra of isotactic polypropylene fibers annealed at 60°C for 45 min. (a) Polarization vector parallel to the fiber axis; (b) polarization vector perpendicular to the fiber axis. [Color figure can be viewed in the online issue, which is available at wileyonlinelibrary.com.]

crystallized. On the other hand, with increasing molecular weight, the crystallinity seems to follow a decreasing trend due to the occurrence of crystallization in a more disordered fashion.

Infrared orientation measurements

Detailed analysis of the polarized infra-red spectra of annealed isotactic polypropylene fibers has been carried out to follow the changes in the molecular orientation which may be taking place during the annealing process as a function of annealing time. The IR peaks around 998, 899, 841, and 809 cm^{-1} are the characteristic regularity bands arising from the presence of helical chains.[56] In the infrared spectrum of amorphous polypropylene, the intensity of the regularity bands are usually very weak or totally absent, which should provide some ideas about the possible molecular changes take place during the annealing process.

Figure 12 shows clearly the polarization directions of the regularity peaks (998, 899, 841, and 809 cm^{-1}) in the 1025–775 cm^{-1} spectral region. In many cases, due to their close proximity to each other, the IR bands at 998, 973, and 841 cm^{-1} are used for the quantitative measurement of the crystalline and the average orientation parameters.[45] The main IR peaks located at 998, 973, and 841 cm^{-1} show parallel polarization characteristics whereas the IR peaks located at 940, 899, and 809 cm^{-1} show perpendicular polarization characteristics (Fig. 12). 998 and 841 cm^{-1} IR peaks are usually assigned to the crystalline phase, whereas the 973 cm^{-1} band is assigned to both the crystalline and the amorphous chains in helical conformations which can be considered as an average band.[39]

The orientation parameters calculated using the regularity band at 841 cm^{-1} for isotactic polypropylene films showed good agreement and correlation with the X-ray diffraction measurements.[45] It was suggested that in the absence of X-ray diffraction data this peak may be used for the determination of the crystalline orientation parameter. This peak has been attributed to long and regular helical chains, most of these chains are likely to be present in the crystalline regions.[56]

The molecular orientation parameters, $<P_2>$ evaluated for the 998, 973, and 841 cm^{-1} peaks using the eqs. (7) and (8) are shown in Figure 13. Transition moment angle for these peaks are taken as[61] 0°.

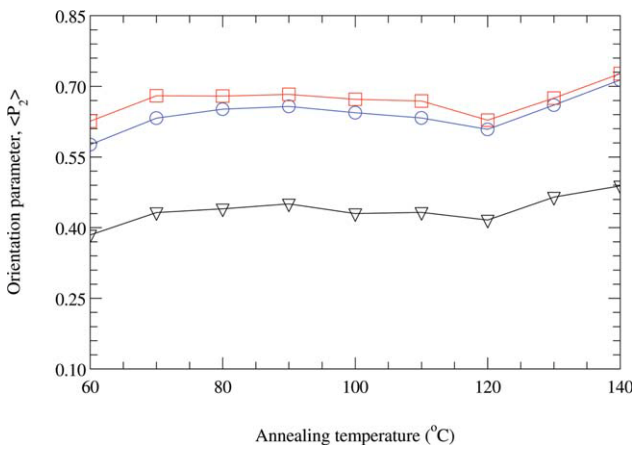

Figure 13 Comparison of the values of the orientation parameter ($<P_2>$) obtained from the 998 cm^{-1} (○), and 973 cm^{-1} (▯) and 841 cm^{-1} (□) infrared peaks. [Color figure can be viewed in the online issue, which is available at wileyonlinelibrary.com.]

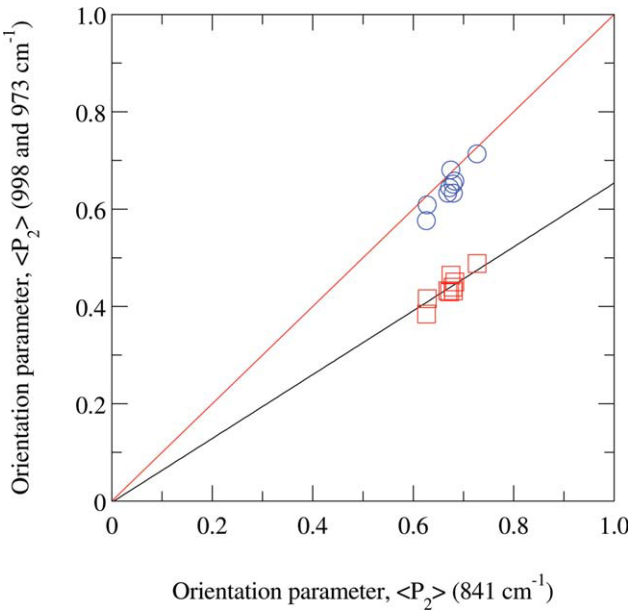

Figure 14 Comparison of the values of the orientation parameter ($<P_2>$) obtained from the 841 and 998/973 cm^{-1} infrared peaks: 998 cm^{-1} (○); and 973 cm^{-1} (□). [Color figure can be viewed in the online issue, which is available at wileyonlinelibrary.com.]

The results show that the values of the molecular orientation parameter corresponding to the crystalline phase arising from the dichroic behavior of the peaks at 998 and 841 cm^{-1}, show a sharp rise from the annealing temperature of 60–70°C followed by a monotonous continuation without much change in the values of the orientation parameters until the annealing temperature of 120°C, after which a steep rise in molecular orientation occurs again until the annealing temperature of 140°C.

In general, the values of the orientation parameter, $<P_2>$, obtained from the 998 cm^{-1} peak are found to be slightly lower than those obtained from the 841 cm^{-1} peak (Figs. 13 and 14).

This result is thought to be in agreement with the assumption that this band contains the absorption direction parallel to the chain axis for highly ordered structure but is likely to be sensitive to less ordered structure.[45]

The values of the orientation parameter corresponding to the 973 cm^{-1} peak containing the components from the crystalline and amorphous phases are found to be significantly lower than those obtained from the IR bands at 998 and 841 cm^{-1} (Figs. 13 and 14).

To evaluate the orientation parameter of the amorphous phase, the band at 973 cm^{-1} was split into the 972 cm^{-1} component assigned to the crystalline phase and the 974 cm^{-1} component assigned to the amorphous phase using the curve fitting procedure detailed earlier in the 1025–923 cm^{-1} spectral range (Fig. 10). Although the IR band at 973 cm^{-1} was resolved into two components, it was assumed that both of these components were due to the same vibrational mode.[45] Painter et al.[55] showed using difference spectroscopy that the 972 cm^{-1} peak is attributed to ordered structure and the 974 cm^{-1} peak is attributed to disordered structure.

Figure 15 shows the values of the orientation parameter, $<P_2>$, obtained from the 974, 972, and 973 cm^{-1} peaks against the $<P_2>$ values obtained from the 841 cm^{-1} peak. The behavior of the 972 cm^{-1} peak is found to be similar to that of the 841 cm^{-1} peak. The 974 cm^{-1} peak is attributed to the amorphous phase and the values of the orientation parameters obtained from this peak are, as expected, lower than those obtained from the 972 cm^{-1} peak attributed to the crystalline phase and the 973 cm^{-1} peak attributed to the average of the crystalline and the amorphous phase contributions.

During the determination of the orientation parameters using the infrared spectroscopy approach, the semicrystalline structure is assumed to consist of only crystalline and amorphous phases and no allowances were made for the smectic phase. This is mainly due to the difficulties in the separation of the infrared vibrations due to the crystalline and smectic forms.

Mechanical properties

The measurement of mechanical properties of fibers are regarded to be an important characteristic

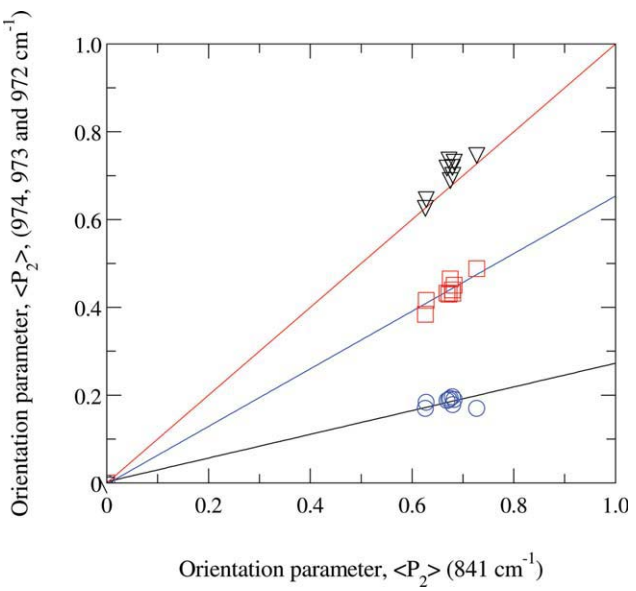

Figure 15 Comparison of the values of the orientation parameter ($<P_2>$) obtained from the 841 cm^{-1} infra-red peak with those obtained from the 974 cm^{-1} (○), 973 cm^{-1} (□) and 972 cm^{-1} (▽) infra-red peaks. [Color figure can be viewed in the online issue, which is available at wileyonlinelibrary.com.]

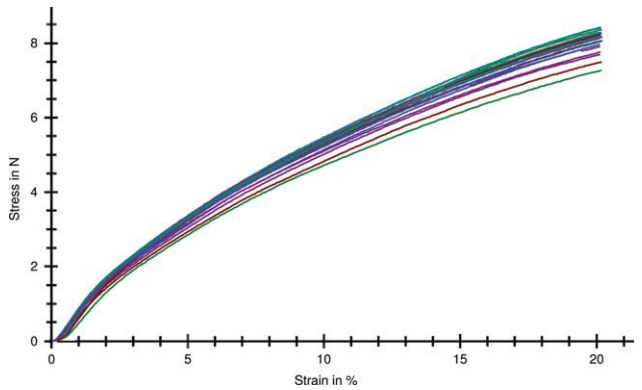

Figure 16 Stress–strain curves of isotactic polypropylene fibers annealed at 60°C for 45 min.[Color figure can be viewed in the online issue, which is available at wileyonlinelibrary.com.]

determining the behavior of fibers during the processing and the performance of the final product.[62]

Figure 16 shows the stress–strain curves for annealed isotactic polypropylene fibers annealed at 60°C for 45 min. Figure 17 presents the effect of the annealing temperature on the tensile strength and elongation at break of annealed isotactic polypropylene fibers as a function of annealing temperature. The values of the tensile strength are found to increase up to the annealing temperature of 130°C followed by a small decrease at the annealing temperature of 140°C. The small decrease in the tensile strength at 140°C may be due to an oxidation related thermal degradation which may have caused small amount of chain scission and the eventual occurrence of tensile strength loss.

Annealing treatment resulted in an increase of tensile strength possibly due to the increase of the density, enhanced crystallinity and increased crystallite size of the annealed fibers. Figure 18(a) shows the correlation of the tensile strength with the degree of crystallinity obtained from the density measurements. These values fall on a straight line, although there is some scatter, indicating that there is a close relationship between the tensile strength and the

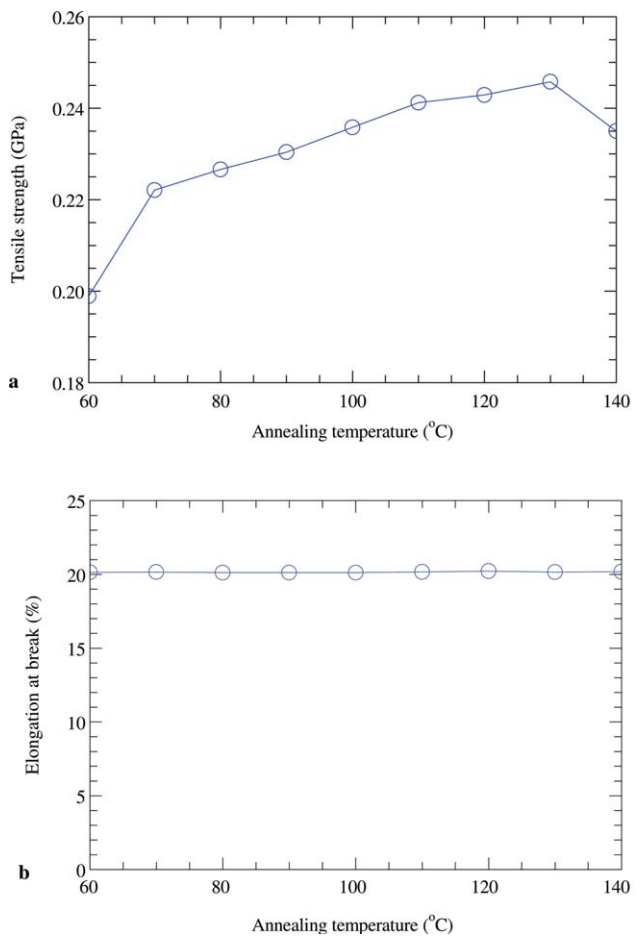

Figure 17 Variation of tensile strength (a) and elongation at break (b) of annealed isotactic polypropylene fibers as a function of annealing temperature. [Color figure can be viewed in the online issue, which is available at wileyonlinelibrary.com.]

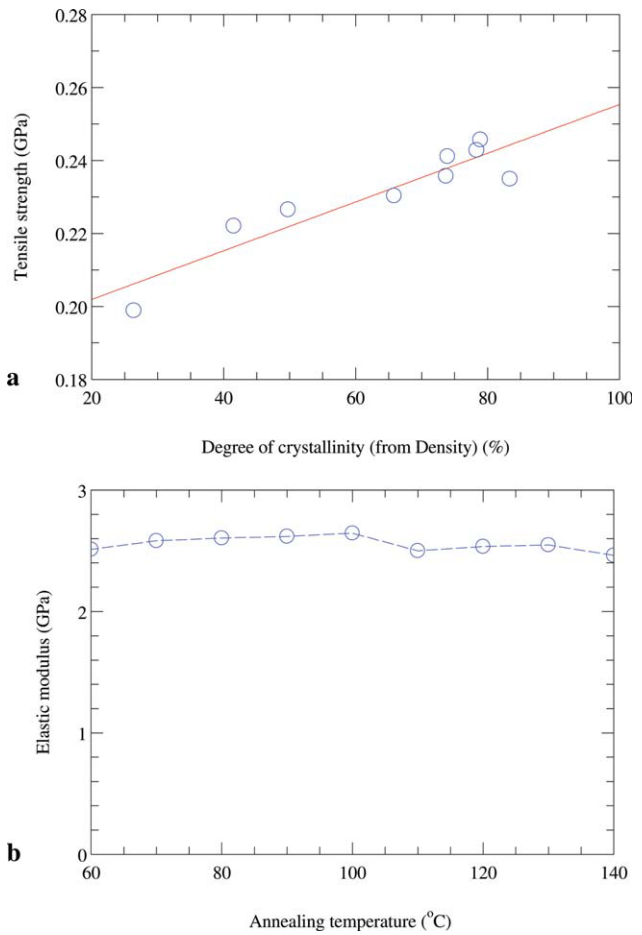

Figure 18 (a) Correlation of the tensile strength with the degree of crystallinity obtained from the density measurements. (b) Variation of elastic modulus of annealed isotactic polypropylene fibers as a function of annealing temperature. [Color figure can be viewed in the online issue, which is available at wileyonlinelibrary.com.]

degree of order developed as a result of the annealing process.

The values of the elastic modulus do not seem to change much [Fig. 18(b)]. This is not surprising because the tensile modulus mainly depends on the molecular alignment along the fiber axis. As mentioned before, during the annealing process, the values of the orientation parameters did not change considerably which indirectly reflects the unchanging nature of the tensile modulus as a function of the annealing temperature. Although there will be some molecular motion during the annealing process, this will not be sufficient to increase the alignment of the polymer chains to a considerable extent. Therefore, significant increases in the molecular orientation are not expected during the annealing process.

Kitao et al.[63] and Sarkeshick et al.[64] reported the decrease of the tensile strength and the elastic modulus of the heat-set isotactic polypropylene fibers as a result of the annealing in the temperature range of 120–150°C[64] and at 140°C.[63] It seems that Sarkeshick et al.[64] carried out heat-setting under relaxed condition rather than under constant length, which seems to have caused some loss of molecular orientation as a result of the physical shrinkage taken place during the heat setting process. In the case of the heat setting reported by Kitao et al.[63] no mention was made about the heat setting procedure.

CONCLUSIONS

An in depth study was performed on the influence of the annealing treatment on the molecular structure and the mechanical properties of isotactic polypropylene fibers annealed in an air heated environment at temperatures ranging from 60 to 140°C. Analysis of the equatorial X-ray diffraction traces showed the presence of a polymorphic system and exhibited the transformation of the smectic form to the monoclinic form with increasing annealing temperature, which resulted in an enhancement of the degree of crystallinity and the crystallite dimensions. Enhancement in the degree of crystallinity and the crystallite size was shown to be more remarkable above 120°C.

Determination of the degree of crystallinity was performed using an analysis of density, infrared spectroscopy and X-ray diffraction methods. Polarized infra-red spectroscopy measurements were utilized for the determination of the isotacticity fractions obtained from the absorbance ratios of A_{998}/A_{973} and A_{841}/A_{973}. Polarized infrared spectroscopy was also used for the determination of the molecular orientation parameters for the crystalline and the amorphous phases. The results showed a slight increase of the molecular orientation of the helical chain segments present in the crystalline phase represented by the IR bands at 841 and 998 cm^{-1} whereas the amorphous structure represented by the IR band at 974 cm^{-1} showed no significant changes with increasing annealing temperature. The improvement in the molecular orientation of the crystalline phase became more remarkable above 120°C.

Mechanical properties, in particular, the tensile strength, of the annealed fibers showed good correlation with the microstructural parameters, such as, the degree of crystallinity. The values of the tensile strength are found to increase with increasing annealing temperature as a result of the increasing density, improvements in the perfection of the crystallites, crystallinity and the lateral crystallite size.

The assistance and the cooperation of Boyteks A.Ş. (Kayseri) is gratefully acknowledged for the extrusion of the polypropylene multifilaments.

References

1. Addink, E. J.; Beintema, J. Polymer 1961, 2, 185.
2. Turner-Jones, A.; Aizlewood, J. M.; Beckett, D. R. Makromol Chem 1964, 75, 134.
3. Danusso, F. Polymer 1967, 8, 281.
4. Natta, G.; Corradini P. Nuovo Cimento 1960, 15, 40.
5. Keith, H. D.; Padden, F. J., Jr.; Walter, N. M.; Wyckoff, H. W. J Appl Phys 1959, 30, 1485.
6. Shangguan, Y.; Song, Y.; Peng, M.; Li, B.; Zheng, Q. Eur Polym Mater 2005, 41, 1766.
7. Tjong, S. C.; Shen, J. S.; Li, R. K. Y. Polym Eng Sci 1996, 36, 100.
8. Li, X.; Hu, K.; Ji, M.; Huang, Y.; Zhou, G. J App Polym Sci 2002, 86, 633.
9. Li, J. X.; Cheung, W. L.; Jia, D. Polymer 1999, 40, 1219.
10. Karger-Kocsis, J.; Varga, J. J Appl Polym Sci 1996, 62, 291.
11. Chen, H. B.; Karger-Kocsis, J.; Wu, J. S.; Varga, J. Polymer 2002, 43, 6505.
12. Morrow, D. R.; Newman, B. A. J Appl Phys 1968, 39, 4944.
13. Sauer, J. A.; Pae, K. D. J Appl Phys 1968, 39, 4959.
14. Angelloz, C.; Fulchiron, R.; Douillard, A.; Chabert, B.; Fillit, R.; Vautrin, A.; David, L. Macromolecules 2000, 33, 4138.
15. Mezghani, K.; Phillips, P. J Polym 1995, 36, 2407.
16. Dean, D. M.; Register, R. A. J Polym Sci Polym Phys 1998, 36, 2821.
17. Perez, E.; Zucchi, D.; Saachi, M. C.; Forlini, F.; Bello, A. Polymer 1999, 40, 675.
18. Meille, S. V.; Brückner, S.; Porzio, W. Macromolecules 1990, 23, 4114.
19. Cocorullo, I.; Pantani, R.; Titomanlio, G. Polymer 2003, 44, 307.
20. Miller, R. L. Polymer 1960, 1, 135.
21. Fujiyama, H.; Awaya, H.; Azuma, K. J Polym Sci Polym Lett 1980, 18, 105.
22. Gailey, J. A.; Ralston, R. H. SPE Trans 1964, 4, 29.
23. Murthy, N. S.; Minor, H.; Bednarczyk, C.; Krimm, S. Macromolecules 1993, 26, 1712.
24. Ferrero, A.; Ferracini, E.; Mazzavillani, A.; Malta, V. J Macromol Sci Phys 2000, B39, 109.
25. McAllister, P. B.; Carter, T. J.; Hinde, R. M. J Polym Sci Polym Phys 1978, 16, 49.

26. Natta, G. Makromol Chem 1960, 35, 94.
27. Hosemann, R. Acta Cryst 1951, 4, 520.
28. Corradini, P.; Petroccone, V.; De Rosa, C.; Guerra, G. Macromolecules 1986, 19, 2699.
29. Corradini, P.; De Rosa, C.; Guerra, G.; Petroccone, V. Polym Commun 1989, 30, 281.
30. Grebowicz, J.; Lau, J. F.; Wunderlich, B. J Polym Sci Polym Symp 1984, 71, 19.
31. Sheehan, W. C.; Cole, T. B. J Appl Polym Sci 1964, 8, 2359.
32. Wang, I. C.; Dobb, M. G.; Tomka, J. G. J Text Inst 1995, 86, 383.
33. Wang; I. C.; Dobb, M. G.; Tomka, J. G. J Text Inst 1996, 87, 1.
34. Natta, G. J Polym Sci 1955, 16, 143.
35. Natta, G.; Pino, P.; Corradini, P.; Danusso, F.; Mantica, E.; Mazzanti, G.; Moraglio, G. J Am Chem Soc 1955, 77, 1708.
36. Hindeleh, A. M.; Johnson, D. J.; Montague, P. E. In Fibre Diffraction Methods, ACS Symp. No. 141; French, A. D., Gardner, K. H., Eds.; American Chem Society: Washington DC, 1983; p 149.
37. Hindeleh, A. M.; Johnson, D. J. Polymer 1978, 19, 27.
38. Stokes, A. R. Proc Phys Soc 1948, A166, 382.
39. Tadokoro, H.; Kobayashi, M.; Ukita, M.; Yasufuku, K.; Murahashi, S.; Torii, T. J Chem Phys 1965, 4, 1432.
40. Karacan, I.; Bower, D. I.; Ward, I. M. Polymer 1994, 35, 3411.
41. Quynn, R. G.; Riley, J. L.; Young, D. A.; Noether, H. D. J Appl Polym Sci 1959, 22, 166.
42. Karacan, I. Fibers Polym 2005, 6, 186.
43. Karacan, I. J Appl Polym Sci 2006, 100, 142.
44. Nielsen, A. S.; Batchelder, D. N.; Pyrz, R. Polymer 2002, 43, 2671.
45. Karacan, I.; Taraiya, A. K.; Bower, D. I.; Ward, I. M. Polymer 1993, 34, 2691.
46. Purvis, J.; Bower, D. I. J Polym Sci Polym Phys 1976, 14, 1461.
47. Karacan, I. J Appl Polym Sci 2006, 101, 1317.
48. Zanetti, R.; Celotti, G.; Fichera, A.; Francesconi, R. Makromol Chem 1969, 128, 137.
49. Nadella, H. P.; Spruiell, J.; White, J. J App Polym Sci 1978, 22, 3121.
50. Radhakrishman, J.; Ichikawa, K.; Yamada, K.; Toda, A.; Hikosaka, M. Polymer 1998, 39, 2995.
51. Vittoria, V.; Olley, R. H.; Bassett, D. C. Colloid Polym Sci 1989, 267, 661.
52. O'Kane, W. J.; Young, R. J.; Ryan, A. J.; Bras, W.; Derbyshire, G. E.; Mant, G. R. Polymer 1994, 35, 1352.
53. Poddubny, V. I.; Lavrentyev, V. K.; Sidorovich, A. V.; Baranov, V. G. Acta Polym 1982, 33, 483.
54. Jasse, B.; Koenig, J. L. J Macromol Sci Rev Macromol Chem 1979, C17, 61.
55. Painter, P. C.; Watzek, M.; Koenig, J. L. Polymer 1977, 18, 1169.
56. Kissin, Y. V.; Tsvetkova, V. I.; Chirkov, N. M. Eur Polym Mater 1972, 8, 529.
57. Zhu, X.; Yan, D.; Yao, H.; Zhu, P. Macromol Rapid Comm 2000, 21, 354.
58. Zerbi, G.; Gussoni, M.; Ciampelli, F. Spectrochim Acta A Mol-Spec 1967, 23, 301.
59. Kobayashi, M.; Akita, K.; Tadokoro, H. Makromol Chem 1968, 118, 324.
60. Greko, R.; Ragosta, G. J Mater Sci 1988, 23, 4171.
61. Gupta, M. K.; Carlsson, D. J.; Miller, D. M. J Polym Sci Polym Phys 1984, 22, 1011.
62. Morton, W. E.; Hearle, J. W. S. Physical Properties of Textile Fibres; Butterworth and Co. (Publishers) Ltd. and the Textile Institute; Manchester, 2008.
63. Kitao, T.; Spruiell, J. E.; White, J. I. Polym Eng Sci 1979, 19, 761.
64. Sarkeshick, S.; Tavanai, H.; Zarrebini, M.; Morshed, M. J. Text Inst 2009, 100, 128.